Arab Institute of Navigation
Cross Road of Sebaei Street & 45 St., Miami, Alexandria, Egypt
Tel: (+203) 5509824
Cell: (+2) 01001610185
Fax: (+203) 5509686
E-mail: ain@aast.edu
Website: www.ainegypt.org

Journal of
The Arab Institute of Navigation
Semi Annual Scientific Journal
Issue 44 (volume 2) July 2022
ISSN (2090-8202)
INDEXED IN (EBSCO)

Contents

Numerical Modeling for Tidal Characteristics and Datum Calculation from Sea Level Simulation in Al-Ahmadi Harbor, Kuwait.

Prepared by

Ahmed M.Khedr 1 *, Mohamed Mohsen 2 , Mostafa Rabah 2 and Fahmy Abd Elhaleem 2

1. College of Maritime Transport and Technology, Arab Academy for Science, Technology and Maritime Transport,

2. Benha University, Faculty of Engineering, Civil Engineering Department, Benha, Qalyubia,

Egypt.

المستخلص:

تعتبر قياسات مستوى سطح البحر أحد أهم المتغيرات في علم المحيطات الفيزيقية، بجانب أهميته فى عمليات المساحة البحرية، وذلك لتحديد مستوى اساس الخريطة. يعتبر أقل مستوى مدرى فلكى بمثابة السطح الفيزيائى والذى يعد أكثر المستويات الرأسية استخدامًا في الآونه الأخيرة من قِبل المنظمة الدولية للمساحة البحرية والتي قامت بتعريفه علي أنه أقل مستوى مدرى يمكن أن يصل إليه مستوى سطح البحر تحت تأثير ظروف مناخية متوسطة وتحت التأثير المشترك للقوى المدرية الفلكية. فى هذا البحث تم تعديل حساب و تعريف أقل مستوى مدرى فلكى على اساس أنه المستوى المدرى الرأسى الذى يتم إسناد الاعماق اليه على الخرائط الملاحية البحرية فى عمليات المساحة البحرية، ويعد الهدف الرئيسي من هذا البحث هو حساب ارتفاع مستوي الاسناد الملاحي من متوسط منسوب سطح البحر بميناء الأحمدي بالكويت. تم الحصول علي قياسات مستوى سطح البحر عن طريق حساس ضغط المياه المثبت على جهاز قياس التيارات البحرية، والذي تم استخدامه في تمثيل سطح البحر عن طريق برنامج النمذجه العددية الهيدروديناميكية للحصول علي مستوي الاسناد الملاحي. تم رصد كلا البيانات (المرصودة – الممنذجة عدديا)، ثم تحليلهم بواسطة التحليل التوافقى البسيط لفصل المركبات المدرية عن المركبات غير المدرية وذلك لتحليلها. من نتائج التحليل لكلًا من سطح البحر المقاس وسطح البحر الي تم تمثيله تم حساب معامل الارتباط، ووجد أن هناك معامل ارتباط كبير بين المركبات المدرية من تحليل منسوب سطح البحرلكلا البيانات المرصودة والممثلة بالمنطقة تصل إلى 97.93 %، بينما اظهرت النتائج وجود علاقة توافق كبيره بين مركبات سطح البحرالمتبقية (الناتجة عن جميع العوامل عدا العوامل المدرية) بنسبة معامل تصل الى 98.06%. وعلاوة علي ذلك، أثبت التحليل التوافقي البسيط أن المركبات المدارية النصف يومية واليومية هي المركبات الأكثر سيطره وشيوعا والأكثر تأثيرًا في المنطقة. وعلاوة علي ذلك، ومن نتائج التحليل التوافقى البسيط تم تصنيف المدر والجزر في المنطقة أنه مدر نصف يومي مختلط وذلك بحساب قيمته من معامل التكوين، والذي حقق 0.85، والذى توافق مع نتائج الدراسات السابقه التي استخدمت نموذج سطحي لتمثيل المياه ونموذج محيطي ثلاثي الأبعاد. تم حساب نسبة عدم التوافق للمدر والجزر والتي تعتبر من أهم العوامل التي تعبر عن حركة الترسيبات في الميناء، و كانت النسبة 0.0191 و 0.0193 بالترتيب لكل من بيانات سطح البحر المقاسة والممثلة بالترتيب، وتشير هذه النسبة الي وجود تشوه في موجه المدر والجذر في منطقة الدراسة مع زيادة

حركة الجذر والتى تؤدى الى خروج الترسيبات من الميناء. واخيرا، من نتائج حسابات أقل منسوب مدرى فلكى لاستخدامه كأساس للخريطة البحرية لكلا البيانات (المرصودة والممثلة) والخاصة بمستوى سطح البحر، وجد أن السطح بقيمة 1.57 م تحت متوسط منسوب سطح البحر والذي يعد اكبر عمقًا من المستوي المحسوب بقيمة لا تقل عن (5 سم) عن طريق مجموعه مساحه النفط الأوروبيه أثناء إنشاء الميناء عام 2004.

Abstract:

Sea level as a major oceanographic parameter is always needed in the field of hydrographic surveying for Chart Datum (CD) realization. Lowest Astronomical Tide (LAT) is a physical surface and the most recent used tidal datum as defined by the International Hydrographic Organization (IHO); "The lowest tidal level may occur under average meteorological conditions and under combination of any astronomical conditions" (IHO, 2011). It was adopted to be used as the vertical tidal datum for depths reduction on nautical charts. In the current paper, the main objective is to calculate the height of (LAT) referred to the mean sea level in Al-Ahmadi harbor, Kuwait. Sea level data were measured by sea level sensors using offshore Acoustic Doppler Current Profiler (ADCP). Simulated sea level time series was acquired from Delft-3D hydrodynamic model, and then it was used for chart datum calculation.Both observed and modeled sea level series were analyzed using harmonic analysis technique, to separate tidal from non-tidal components. Results of both data sets modeled and observed (tidal and non-tidal signals) were cross-correlated for model validation. Results showed a strong direct correlation between both tidal and residual components from both data sets by 97.93 % and 98.06 % respectively. Furthermore, from harmonic analysis it was found that M2 (Principal lunar semi diurnal), K1 (principal luni-solar diurnal), O1 (principal lunar diurnal) and S2 (Principal solar semi diurnal) are the most significant and dominant tidal constituents in the area. Moreover, tidal type regime Form Factor (FF) ratio shows a mixed semi-diurnal tidal regime by (0.85). These outcomes agree with the results obtained by (Pous, 2012; and Akbari, 2016) using shallow water model and 3D coastal ocean model respectively, for the same area. The tide asymmetry ratio, which is regarded as the major representation of harbor sediment transport, was 0.0193 and 0.0191, respectively, for both observed and modeled datasets, indicating that there is a distortion in tide wave in the area, with ebb-dominant outflow sediment transport away from the harbor. Finally, from modeled sea level dataset, LAT as Chart-datum in the area was found (1.57 m) below Mean Sea Level (MSL), which is higher thanthe one calculated by the European Petroleum Survey Group (EPSG 5188) during mina Al-Ahmadi refinery construction in 2004 by (5 cm).

Keywords: (Modeled Sea level, Delft-3D flow, tidal datum, LAT and HAT, MACD).

1- Introduction

The Arabian Gulf and its coastal areas are the world's largest single source of crude oil and related industries which dominate the region. The rapidly increasing needs to explore, drill and transfer oil and gas leaded to enormous acquirements of high quality hydrographic and hydrodynamic researches. Arabian Gulf is considered a semi-enclosed basin connected to the deep Gulf of Oman through Strait of Hormuz (Johns et al., 2003). Al-Ahmadi harbor is located at the southeastern part of Kuwait at the position (29.0696°N, 48.1789°E) as shown in Figure (1), and it's considered the principal harbor for crude exports product and gas. The refinery and harbor are located 45 kilometers south of Kuwait City on the Arabian Gulf. This coastal zone has a tremendous effect on global economy, due to its rich resources of gas and oil, which made it one of the critical waterways in the world. Due to this importance, Arabian gulf generally and Kuwaiti harbors specifically have subjected to several studies and master development plans.Nevertheless, there is still a need for more oceanographic and hydrographic studies especially in the discipline of sea level.

Figure 1. Location of the study area located on the Persian Gulf.

As a result of global warming and its effect on sea level, it became a field of several studies (Al- Jeneid et al., 2008). Consequently, global Sea level rose rapidly by about 3.1 mm per year from 1993 to 2003, as compared to the average rate of 1.8 mm per year from 1961 to 2003 (IPCC, 2007), Church and White in 2011, estimated the increase of Global Mean Sea Level (GMSL) from 1880 to 2009 was 21 cm, the rate of (SLR) was 3.2 ± 0.4 mm/year (1993 to 2009), then (1900 to 2009) as 1.7 ± 0.2 mm/year which shows twice the value. While, sea level value varied in the northwest part of the Arabian gulf. Several researches were made in the area using sea level data observed from 2 tide gauges. Sultan et al., (1995) concluded in their results from 10 years (1980-1990) that (SLR) is constant by about 2.1 ± 0.1 mm per year. A rate of 2.34 ± 0.07 mm per year was announced by (Hosseinibalam et al.2007) using 9 years of observed data (1990-1999).

Precise determination of LAT referenced to (MSL) in Al-Ahmadi harbor has to cope with the new advanced charting technology to fulfill the most recent LAT definition of the (IHO). The technical resolution of the IHO stated that LAT should be adopted as (CD), where tides have a considerable effect on the water level. The chart datum was chosen as a surface that is so low that the tide will not frequently fall belowit, not so low as to be unrealistic and only gradually varying between adjacent datum (FIG,2011).

Delft3D-FLOW model is a progressive combined computer software that carries out model of unsteady flow and transport processes that outcomes from tidal and non-tidal meteorological forcing on a well fitted rectilinear boundary grids (Delft-3D, 2014).Delft-3D is a program consists of numerous modules, each module covers a varied series of aspects, clustered around a reciprocated interface, capable of interrelate with one another, each module can be implemented autonomously or in association with other modules.

This (CD) needs to be re-calculated and updated regularly as a consequence of (SLR), using continuous measured sea level data. So, according to what mentioned, and due to the scarcity of observed data, a consistent and continuous modeled sea level data for 19 years was accounted to replace the observed data. For the purpose of nautical chart production, thisdata should be validated and analyzed verycarefully (Baqer et al., 2011), to providestakeholders with a complete description of tidaldatum for the right decision for the future plans. In this study, a 2-diminsional hydrodynamic model by Delft-3D was implemented to simulate sea level using the flow module in Al-Ahmadi

harbor. Water level time series was acquired and validated using observed sea level data from an (ADCP) with sea level sensor. Harmonic analysis was executed for both observed and simulated time series to get the significant and dominant constituents in the area of study. This research article aims to precisely update and re-define the Kuwaiti tidal (CD), applicable in the area in front Al-Ahmadi harbor on the Arabian gulf. The main objective of this study is to establish an approximate and quick Tidal Level (TL) for hydrographic surveying process and dredging works using short-term modeled offshore sea level data after being validated by observed sea level data.

2. Data and Methods of Analysis

2.1. Data

The available data used for this study were classified as follows:

2.1.1. Observed sea level:

Although the available observed sea level data is not adequate enough for accurate tidal datum calculation, it was used for model validation and boundary condition. Observed sea level data in this paper acquired from two offshore (ADCP, Nortek Aqua dopp) with 15-minutes time step (from 7th of December, 2019 till 7th of January, 2020), and it was divided according to the location as depicted in Figure (2) as follow;

A- Sensor "A" deployed at a depth of 10.8 relative to (MACD), at the geographical position (29°04'02.7"N 48°09'24.7"E) that was the first data set through which the simulated sea level data at the same location was compared, cross correlated and validated.

B- Sensor B deployed at a depth of 4.2 relative to (MACD), at the geographical position (29° 4' 27.7" N, 48° 9' 15.9" E) that was the second observed sea level data set by which the flow model boundary condition was created.

Figure 2. Location of ADCP sensors located in AL-Ahmadi harbor, Kuwait.

2.1.2. Meteorological Parameters:

A 1-minute time step weather data from (1st of June, 2019 till 2nd of February, 2020), including both wind speed and direction, surface temperature and atmospheric pressure, which was recorded for further computations and accurate flow simulation modeling.

2.1.2. Bathymetric data:

Bathymetric data in Easting, Northing anddepths (X, Y, Z) file format was acquired during a hydrographic surveying project, using multi-beam echo sounder (R2Sonic 2024), compiled by HYPACK 2009 a computer software program.

2.2. Methods of Analysis

2.2.1. Observed data smoothing and filtering

One-month of observed sea level data sets with no gaps acquired from (ADCP) were arranged and checked for mistakes, outliers and spikes, then smoothed as shown in Figure (3).

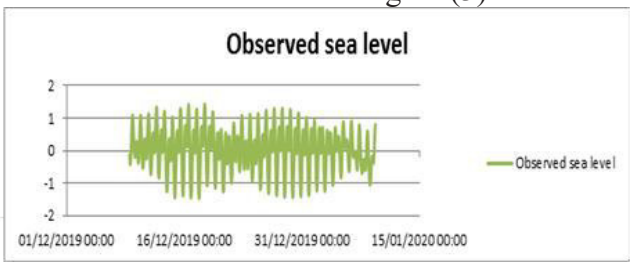

Figure 3: Sensor A and sensor B sea level raw data (from 7th of December, 2019 till 7th of January, 2020) and vertical axis is sea level in meter and thehorizontal one is in days.

As shown in Figure (3), From plotted data it is obvious that the signals display tidal harmonic pattern, which means that tidal components are dominated with slight effect of residuals due to non-tidal parameters such as meteorological parameters.

2.2.2. Hydrodynamic flow simulation

Delft3 D-FLOW model was used to simulate two-dimensional (2D) of one computational layer for unsteady flow inside Al-Ahmadi harbor. Model was initiated using land boundary file drawn by Google earth pro, bathymetric data well fitted and linearly interpolated on a rectilinear grid of the study area as shown in Figure (4). Tide generating

force and meteorological forcing besides the density effect, were used as inputs for the model development.

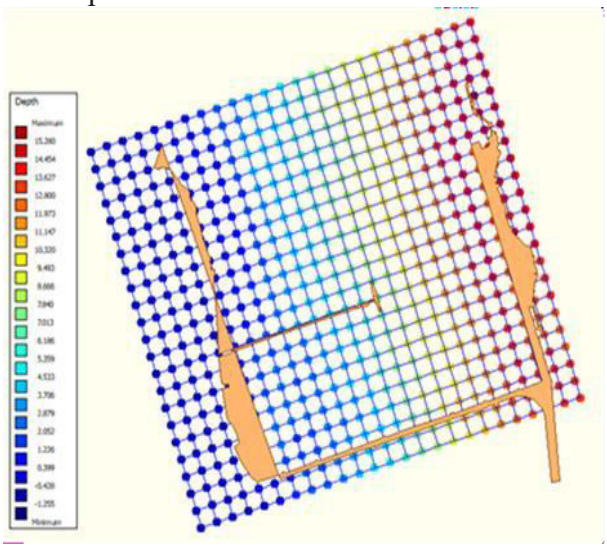

Figure 4. Land boundary file created by Google earth pro, bathymetry file well fitted to the rectilinear grid cell corners created by Delft-3D

The Master Definition File (MDF) was created sensibly starting with collecting attribute files created while initiation such land boundary file for harbor delineation. Rectilinear grid file was built with a grid size (60*60) m2 after being well smoothed and orthogonalized. Bathymetric data file, and other interfaces exist while building (MDF) were represented in the latitude (29.31 deg.) to consider a fixed Coriolis force in the entire area, orientation of the grid cells was (342 deg.) clockwise. Flow simulation duration was one month for the time interval from (7th of December 2019 till 7th of January 2020), and time step 0.15 minute. Thin dams were set in the (eastern, southern and T shape out of shore line of the harbor) as shown in Figure (5) in yellow lines, to prevent flow exchange between the two sides of the harbor. Furthermore, the only open boundary that permits flow to exchange was made in thenorth boundary as shown in Figure (5) with blue line. Boundary conditions were prescribed at the north boundary (Begin and End) points, characterized by the (6, 23) and (25, 23) indices respectively. While values of points that lie inbetween these two points were computed by linear interpolation. Sea level time series from ADCP sensor (B) was used as boundary conditions.

Meteorological effects represented by wind and temperature parameters were taken into consideration as a uniform wind data file. The (MDF) was ready to run after clarifying the monitoring point at ADCP sensor (A) at (16,7) as shown in Figure (5) to check the results.

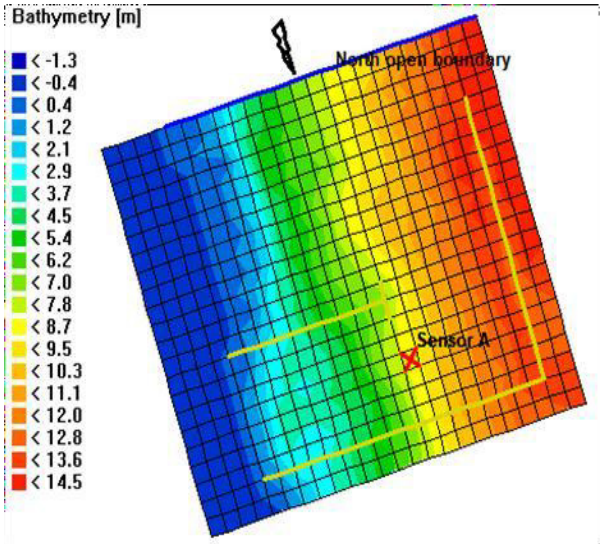

Figure 5. Visualization of all MDF parameters created by Delft 3D flow module

The model was run 2 times, using a laptop(Intel(R) Core(TM) i7-6500U CPU @ 2.50GHz, 2.60 GHz and 8 GB RAM). Using different methods of logging in meteorological parameters inside the (MDF), whether it's a space varying or a uniform wind data file.

1- The first run lasts for 1.5 h, created with a space varying wind and pressure file.
2-The second run, created using a uniform wind data file, and it took about 1.5 h.
The second run showed better results for simulated sea level data, tidal harmonic constants with a high degree of precision when compared with the observed sea level data.

2.2.2. Harmonic analysis

Tidal harmonic technique was used for sea level data analysis to discriminate astronomical tidal constituent heights and its relevant frequencies (Pugh, 2004). Tidal Analysis used iteration procedure which is a trial and error process to calculate amplitudes of each tidal constituent component for frequency and phase. These set of amplitudes and phases decided by the

Analysis are called Tidal Harmonic Location Constants (Pugh, 2004).

By using the results from the analysis, the Mean Sea Level (MSL) for the study area, the chart datum at the area of interest can be realized (Pugh, 2004; Tonbol, 2013; and Khedr et al., 2018). Delft3D-software tide suit converts the data obtainedfrom sensor (A) into tidal harmonic constituents (Bazli, B. H., & Joanes, and J. 2016), by which tide signal can be predicted for any date in the future or in the past (Pugh, 1987; Jorda et al., 2012). Delft-3D is mainly dependent on the concept of expressing the amplitudes of tides atany location as the sum of the whole harmonic constituents (Pugh, 1996), as follows:

$$h_{(t)} = H_0 + \sum_{i=1\ to\ n} f_i\, H_i\, \cos(\alpha_i t + \{V_0 + u\}_i - k_i)$$

Where:

$h_{(t)}$ Tide height at any time t, above a datum.

n : Number of constituents used in tide prediction.

H_0 : The mean sea level above the datum.

H : Amplitude of the tidal constituent.

α_i :Angular speed (degrees/hour) of tidal constituent.

t : The time from initial epoch (hours).

k_i: Tidal constituent epoch relative to the transit of the moon over the location of tide.

f_i: Tidal constituent node factor.

$\{V_0 + u\}$: Tidal constituent equilibrium argument at t = 0 (degrees).

$(\alpha_i t + \{V_0 + u\} - k_i)$: The phase at any time trelative to the transit of the moon.

The obtained heights consist of two components tidal and non-tidal. Astronomical tidal constituents were calculated using least square method in delft-3D then subtracting all astronomical component heights from simulated sea-level heights. Non-tidal components were obtained from the residual signal (Eid, 1990;and Svensson and Jones, 2004).

2.2.2. Model validation

Cross correlation method of analysis was done for model validation, by estimating the relationship between modeled and observed sea level datasets at the same time span. Cross correlation statistical analysis was used to understand the relation between the two independent variables, by exploring the form and strength of this relationship, besides, the time shift for best correlation results. Both data sets, tidal components and the residuals were cross correlated using MATLAB code.

Root mean square error is an analytical expression which is very similar to Standard deviation (SD) in the sense that RMSE refers to N data points instead N-1. RMSE can be Expressed by equation (2).

$$RMSE = \sqrt{\frac{1}{N}\sum_{i=1}^{n}(Oi - Si)^2} \qquad (2)$$

Where:

oi: Observed sea level value

si: Simulated sea level value

N: Number of observed points

RMSE which is considered an evaluation for numerical predictions as a general- purpose error metric, has the same unit of Oi and Si, can sometimes be expressed in.%

2.2.2. Form factor

By using the resultant amplitudes of the four major tidal constituents, tidal cycle type in the area of study was determined using the following form factor equation (Pugh, 2004):

$$F = (H_{O1} + H_{K1})/(H_{M2} + H_{S2}) \qquad (3)$$

Where:

HO1: The tidal amplitude of the principal lunar diurnal constituent.

HK1: The tidal amplitude of the luni-solar diurnal constituent.

HM2: The tidal amplitude of the principal lunar semidiurnal constituent.

HS2: The tidal amplitude of the principal solar semidiurnal constituent.

According to the value of the form factor F, the type of a tidal oscillations may be considered as follows (Pugh, 2004):

The constituent factor F

Range	Tidal cycle type
0 to 0.25	semidiurnal
0.25 to 1.5	mixed semidiurnal
1.5 to 3	mixed diurnal
larger than 3	diurnal

2.2.6. Tide Asymmetry

Asymmetry is frequently defined as the distortion occurred in the tidal wave. Tidal asymmetry is characterized by imbalanced falling and rising tidal periods and unequal peak flood and ebb currents (Pugh, 1987;and Prandle, 1991). According to the results of tidal analysis and in terms of harmonic constituents, tidal asymmetry is reflected by the interaction between M2 and its over-tides such as M4 and M6, which are 2 times and 3 times in frequency of the basic M2 tide (Speer and Aubrey, 1985; Friedrichs and Aubrey, 1988). It has been found that M4 is the main provider for the distortion of tidal wave in this coastal areas (Friedrichs, , 1988). A ratio of M4 and M2 was used for distortion degree expression and asymmetry of the tides.

$$\text{Ar M4} = \frac{\text{M4amp}}{\text{M2amp}} (4)$$

where Ar is the amplitude ratio; Ar M4 > 0.01 indicates a significant distortion in the tide wave.

$$\emptyset M4 = 2\theta M2 - \theta M4 \ (5)$$

Where θ shows the phase. If 0<ØM4<180, the flow is classified as flooding flow. If 180<ØM4<360, the flow is considered as ebb-dominant. This relationship is considered a complete definition of sediment transport. If the harbor is flood- dominant, the transport of sediment is towards the interior of the harbor that lead the decision makers for dredging process from time to time. In contrast, if the harbor is ebb-dominant, sediment tends to be transported out of the harbor (Dias, 2013).

2.2.2. Energy Percentages of both Tidal(TP) and Residual (RP).

Amplitude percentage of both tidal and non-tidal signals were calculated and compared to the sea level absolute value in meters, to acquire amplitude energy percentage of both tidal and non-tidal components. Power percentages of both tidal and residual signals were calculated referred to the total sea level signal using the Formulas (6) and (7), which was written in MATLAB code;

RP % = [MRP / (MRP + MTP)] X 100% (6)

TP % = [MTP / (MTP + MRP)] X 100%(7)

Where: Residual Power Percentage is (RP %), and (MRP) is Mean Residual Power, while (MTP) is the Mean Tidal Power.

2.2.2. Tidal Datum calculations

Tidal datum heights were calculated using the equations figured by (Khedr et al, 2018), using a MATLAB code according to latest (IHO) definition of (LAT) and (HAT).

HAT=0+mean_sea_level+abs(max._ tid._level)+ abs._ average_ resd. (8)

LAT=0+mean_sea_level-abs(min._ tid._ level)-abs._ average_ resd. (9)

Other tidal datum heights were calculated based on the amplitude values of the four major harmonic constituents (M2, S2, K1, O1) acquired from harmonic analysis (Khedr et al, 2018).

The procedure and analysis methods used in this work took into account the following:

1- Available sea level data sets, measured wind data and all (MDF) attribute data files were prepared, filtered and rearranged using Microsoft Excel.

2- Delineation of land boundary of Al-Ahmadi harbor and bathymetric data files filtered and interpolated using Google Earth pro and Hypack 2009a.

3- Flow model simulation was run for extracting simulated sea level data using Delft-3D program flow module.

4- By tide suit Delft-3D, harmonic analysis technique was used to decompose the signal into its two components (tidal– non tidal) components.

5- Using MATLAB Codes for data validation, time lag determination, (PSD)

charting and judging the tidal and non-tidal energy, and tidal datum (most used) calculation (LAT, HAT).

3.Results and discussion

After running the flow model for about one and half hour to simulate sea level time series. A time series of sea level was obtained with time step 15 minute from (from 7th of December, 2019 till 7th of January, 2020) as shown in Figure (6) at the same location of sensor (A).

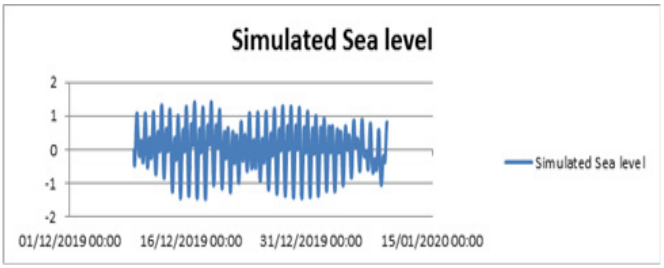

Figure 6. Simulated sea level data at sensor (A) resulted from model simulation from (7th of December, 2019 till 7th of January, 2020).

The resulted simulated sea level signal appeared to be similar to the observed sea level.

2.1. Harmonic analysis

Harmonic analysis used for both data sets, observed and simulated, was made using tide module in Delft 3D. Program algorithm identified amplitudes of 30 tidal components, with only 14 significant constituents that supposed to represent tidal energy in the area of study as shown in Figure(7). Residual components of both data sets were illustrated in Figure (8) after subtracting theharmonic component from the original signal.

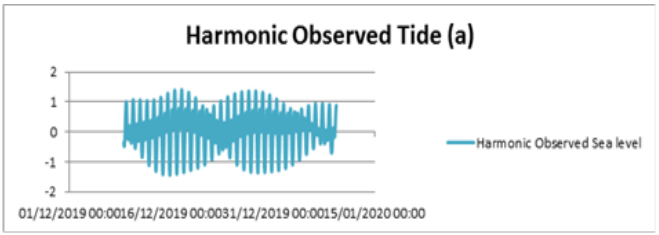

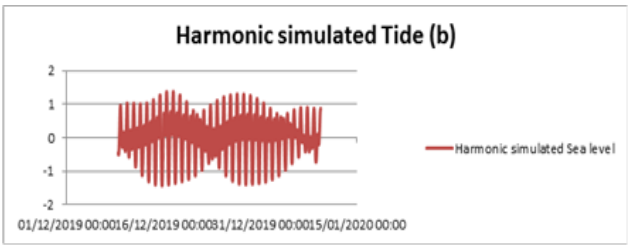

Figure 7: Harmonic component of the significant tidal constituents from the: a) Observed sea level data at sensor (A); b) Simulated sea level data at sensor (B).

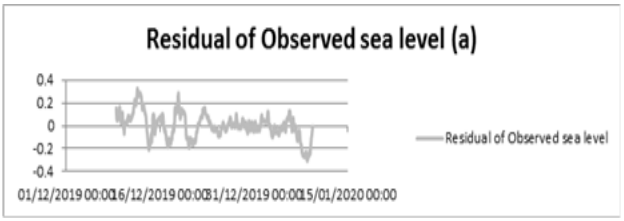

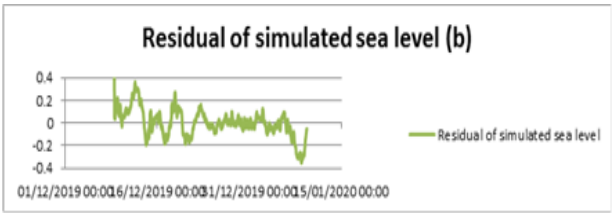

Figure 8: Residual component of the: simulated sea level data sensor (A); simulated sea level data sensor (B).

Table 1. Amplitudes and phase of Significant tidal constituents' parameters from harmonic analysis for simulated and observed data.

constituents	Amplitudes (cm.)			Phase(deg.)	
	Simulated Data	Observed Data	Diff	Simulated Data	Observed Data
M2	62.2	62.7	-0.5	293	307.4
K1	45	45.3	-0.3	120.9	128.5
O1	26.7	27	-0.3	42.9	50.1
S2	21.3	21.4	-0.1	29.1	43.8
P1	14.7	14.9	-0.2	120.9	128.5
N2	11	11.1	-0.1	242.3	256.5
Q1	7.5	7.5	0	20.2	27.7
MFM	6.3	6.4	-0.1	286.2	293
K2	6	6.1	-0.1	29.1	43.8
MK3	4.6	4.8	-0.2	23.1	45
MQM	3.7	3.4	0.3	203.7	209.4
2KO1	3.5	3.6	-0.1	47	55.6
O2	2.6	2.6	0	42.9	57.8
MF	2.3	1.6	0.7	232.3	244.8

Tidal constituents in the diurnal and semi-diurnal bands such as; (K1, P1, O1, M2, S2, K2 and N2) were noticed with almost same amplitudes and phase angles with slight differences in both ranged data sets ranged from 0.7 cm in MF to -0.5 cm in M2 in amplitudes. While the phase differences were within 14 deg. for the significant tidal constituents. The most significant tidal constituents S2, K2, O2 and N2, were matching. The difference between the simulated sea level data and the observed one are smaller than 5%.

Table2. Amplitudes of Significant tidal constituents' parameters from harmonic analysis for both simulated and observed data sets with (FVCOM)

constituents	Simulated Data cm	Observed Data cm	(FVCOM) cm. (Akbari, 2016)
M2	62.2	62.7	63.3
K1	45	45.3	43.2
O1	26.7	27	29.3
S2	21.3	21.4	17.2
P1	14.7	14.9	14.2
N2	11	11.1	12
K2	6	6.1	5.3

For both observed and simulated data harmonic analysis results, a validation of both data sets was given in table (2) with the previous study of Akbari (2016) who used the coastal ocean model (FVCOM). Comparing results showed agreement with the significant tidal constituents with a maximum difference 3.2 cm for S2 and minimum difference of 0.4 cm for K2.

2.2. Cross correlation for model validation

Model results were also validated by available observed sea level data acquired from sensor (A) using a cross-correlation technique as shown in Figure (9). After harmonic analysis by tide module in Delft 3D for both data sets, theharmonic components were cross correlated as shown in Figure (10), furthermore the residual components as shown in Figure (11).

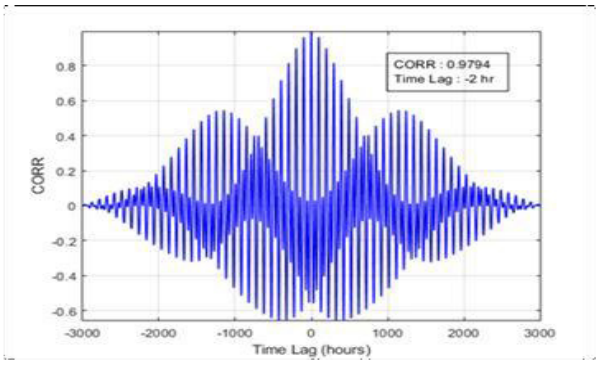

Figure 9. Cross correlation (0.9794) and time lag (-2 hr.) between modeled and observed sea level data sets during the time period (07/12/2019 - 07/01/2020)

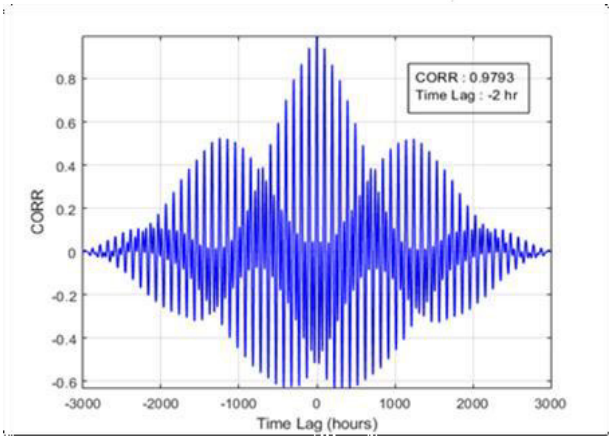

Figure 10. Cross correlation (0.9793) and time lag (-2 hr.) between modeled and observed tidal signals during the time period (07/12/2019 - 07/01/2020)

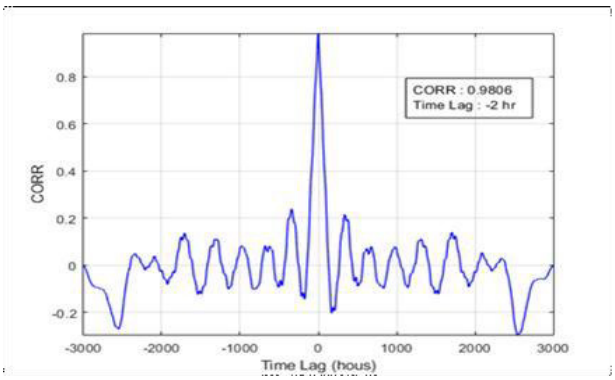

Figure 11. Cross correlation (0.9806) and time lag (-2 hrs.) between modeled and observed residual signals during the time period (07/12/2019 - 07/01/2020)

Fluctuations of both data sets at the same location of Sensor (A) were compared as shown in Figure (9), and it was found that there is a strong direct correlation noticed in the phase of the two tidal signals by approximately (97.94 %), moreover the mean difference

is 0.03 m. Root mean square error was calculated using equation (2) and was found to be 0.13 m, furthermore, in Figure (10), (X corr) between tidal components by (97.93 %), the mean differences is (-0.03 m) and (RMSE) is (0.13 m). While residuals components in Figure (11) shows a value of (98.06 %), and (RMSE) is (0.04 m). The values of cross correlation analysis which is considered a measure of similarity between the two-time series, mean differences and (RMSE) showed good agreement between model results and the observed sea level data.

2.2.Tidal cycle determination

To classify the nature of tide in the study area, the Form Factor was applied by equation (3) and the results are indicated in Table (3).

Table 3. The amplitude of the four major dominant constituents in the area

	Simulated data		Observed data	
No.	Constituents	Amp.(cm)	Constituents	Amp. (cm)
1	O1	26.7	O1	27
2	K1	45	K1	45.3
3	M2	62.2	M2	62.7
4	S2	21.3	S2	21.4

For both observed and simulated data, the tidaltype regime was found to be a mixed semi diurnal as the calculated Form Factor was 0.85which agrees with the results obtained by V.C. John in 1988.

2.2.Tide Asymmetry

Table (4) shows the dominant constituents in sediment transport, by using equation (4) it was found that the amplitude ratio for simulated and observed constituents 0.0193, 0.0191 respectively. Using equation (5) by the given phase shows that 180<ØM4<360.

Table 4. The amplitude and phase of the three dominant constituents in tide asymmetry sensor (A)

	Simulated data			Observed data		
No.	Constituents	Amp. (cm)	Phase (deg.)	Constituents	Amp. (cm)	Phase (deg.)
1	M4	1.2	304.4	M4	1.2	332.8
2	M2	62.2	293	M2	62.7	307.4

According to tide asymmetry and the Ar M4, there is a significant distortion in tide wave. Value of ØM4 is an indication that ebb is dominant in the harbor, which means that transport tends to be out of the harbor.

2.3. Power Spectral Density

The different tidal constituents power could be expressed by its power spectrum. According to harmonic analysis by Delft-3D tide module and the resulted significant constituent's frequencies, it's realized that the highest power peaks are found at the most dominated frequencies affecting the analyzed time series.

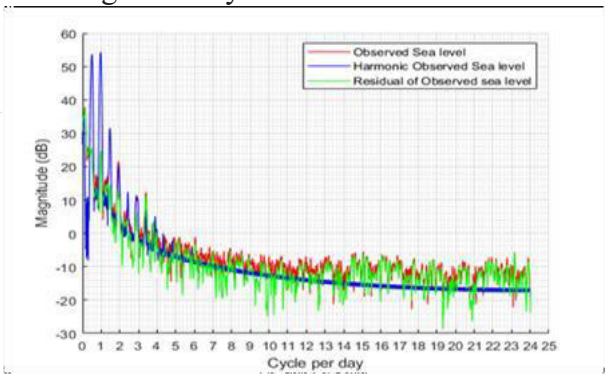

Figure 12. Power spectral density (PSD) showing the observed sea level (red), extracted tidal energy (blue) and residual energy (green) inside Al-Ahmadi harbor (07/12/2019 - 07/01/2020)

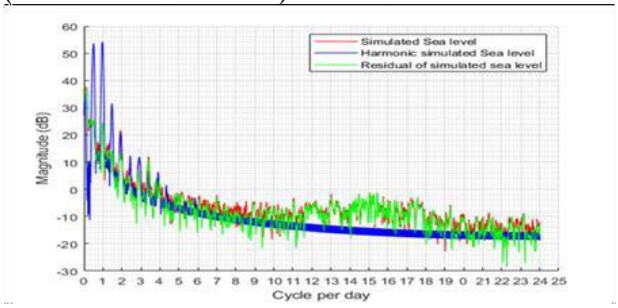

Figure 13. Power spectral density (PSD) showing the simulated sea level (red), extracted tidal energy (blue) and residual energy (green) inside Al-Ahmadi harbor (07/12/2019 - 07/01/2020)

From Figure (12), it appears that the energy peaks coincided with significant frequencies associated with diurnal constituents such as (K1, P1 and O1) and semidiurnal such as (M2, S2, K2 and N2).
Figure (13) shows the same results for simulated sea level data set with diurnal constituents (K1, P1 and O1) and semidiurnal such as (M2, S2, K2 and N2).

2.2. Residual and Tidal Power Percentage

Power percentages of both residual and tidal signals to the total sea level signal were calculated,using the output signals resultant from harmonic analysis. Power percentages have been calculated for both data sets as shown in Table (4).

Table 4. Power percentages of tidal and residual signals to the sea level total signal

Components	Power percentages	
	Observed Sea Level	simulated Sea Level
Residual Power	3.79%	3.34%
Tidal Power	96.21%	96.66%

2.Tidal Datum Calculation.

Even though the ADCP sensor ellipsoidal height is missed. furthermore, the vertical datum definition needs more computations in order to be realized. The Tidal levels well defined by IHO can be calculated using equation (8) and equation (9) which was validated lately by European Petroleum Survey Group (EPSG:5188) that states that (MACD) is 1.52 below (MSL). In this thesis (LAT) and (HAT) were calculated to be 1.57 below (MSL) and 1.52 above (MSL) respectively. Other tidal datum was also computed related to(MSL) following (Khedr et al., 2018) and were as shown in table (5).

Table 5. the values of tidal datum calculated from the simulated sea level data during the period of (07/12/2019 - 07/01/2020)

Tidal datum	value (cm)
(MHWS)	83.5
(MLWS)	-83.5
(MHWN)	40.9
(MLWN)	-40.9
(HHWL)	155.2
(LLWL)	-155.2

4. Conclusions:

The flow model of Delft-3D was proved to be a reliable tool for numerical simulation for flow. Validation of simulated sea level data with observed data set at the same location and same period of time showed a strong X-correlation of about 97.94 % and RMSE 0.13 m. From harmonic analysis by the tide suite Delft-3D, it was noticed that there are 14 significant tidal constituents in the area including the main dominant diurnal and semidiurnal tidal constituents (K1, P1, O1, M2, S2, K2 and N2). Comparing results of both simulated and observed data sets, it's reflected that the main tidal constituents are almost the same with slight differences, even with previous studies by (Pous, 2012; Akbari, 2016). Tidal type regime calculated (FF) value is (0.85) which induced mixed semi-diurnal tidal regime in the area. Tide asymmetry showed a distortion in tidal wave with an ebb tide dominant in the study area. From power spectral density, a significant tidal power was noticed, diurnal and semi- diurnal bands (K1, P1, O1, M2, S2, K2 and N2).From relative power percentage calculations of both tidal and residual signals to the total sea level signal after demeaning both signals, both tidal and residual have almost the same effectsto total sea level. Tidal datum levels were calculated and showed an acceptable value compared with the European Petroleum Survey Group 5188, with a difference of 5 cm.

5. **Recommendations for Future Research**

This work shows a short period flow model simulation, although the flow model results were validated Using statistical methods and previous studies. Observed sea level data for a nodalcycle should be provided for more accurateresults. A continuous update of vertical datumcalculation is needed for tidal datum realizations

For the study area. A wave rider sensor is recommended to be fixed with Acoustic Doppler current profiled to get offshore wave data which can be coupled with Delft-3D flow module to compute the effect of flow on waves. The dominant tidal constituents in the study area can beeasily used for tide prediction.

References

Al-Jeneid, S., Bahnassy, M., Nasr, S., Raey, M.E., (2008) Vulnerability assessment and adaptation to the impacts of sea level rise on the Kingdom of Bahrain. Mitig. Adapt. Strateg. Glob. Change 13: 87-104

Aubrey, D. G., and P. E. Speer (1985), A study of non-linear tidal propagation in shallow inlet/estuarine systems part I: Observations, Estuarine Coastal Shelf Sci., 21: 185-205.

Baqer, M. M., Eman, A., Gopi, S., Renati, K., Al khatib Al., and Subbaraju, K., (2011); "Establishing and Updating Vertical Datum for Land and Hydrographic Surveying in Dubai Emirates", Marine/Coastal Modelling and Technology, FIG Working Week 2011, Bridging the Gap between Cultures, Marrakech, Morocco.
Bazli, B & J., Joanes. (2016). Stream Prediction for Tidal by Algorithm of GeoTide.

Church, J.A., White, N.J., 2011. Sea-level rise from the late 19th to the early 21st century. Surv. Geophys. 32: 585-602
http://dx.doi.org/10.1007/s10712-011-9119-1

Dias J.M., Valentim J.M., Sousa M.C., (2013) A numerical study of local variations in tidal regime of Tagus estuary 8: e80450.
https://doi.org/10.1371/journal.pone.0080450

Eid, F.M., (1990) Variation of surge heights at Alexandria Port (Egypt). Journal King Abdul-Aziz University (JKAU), Marine Science 9: 3-18.

Friedrichs, C.T., Aubrey, D.G. (1988) Non-linear Tidal Distortion in Shallow Well-Mixed Estuaries: A Synthesis. Estuar. Coast. Shelf Sci. 27: 521-545.

Harvey, N. 2005. Review of Changing Sea Levels: Effects of Tides, Weather and Climate, by D. Pugh. Oceanography 18(1):251–252, https://doi.org/10.5670/oceanog.2005.78.

Hosseinibalam, F., Hassanzadeh, S., Kiasatpour, A., (2007) Interannual variability and seasonal contribution of thermal expansion to sea level in the Persian Gulf. Deep Sea Res. I Oceanogr. Res. (54) 1474–1485
http://dx.doi.org/10.1016/j.dsr.2007.05.005

IHO, (2011); "Resolutions of the International Hydrographic Organization Publication M-3", 2nd ed., available at (www.iho.int, 2011b).

IPCC, (2013); "The Physical Science Basis Contribution of Working Group I to the Fifth Assessment", The Climate Change Report of the Intergovernmental Panel on Climate Change [Stocker, T.F., D. Qin, G.-K. Plattner, M.Tignor, S.K. Allen, J. Boschung, A. Nauels, Y. Xia, V. Bex and P.M. Midgley (eds.)], Cambridge University Press, United Kingdom, and New York, USA.

Johns, W. E., F. Yao, D. B. Olson, S. A. Josey, J. P. Grist, and D. A. Smeed (2003) Observations of seasonal exchange through the Straits of Hormuz and the inferred heat and freshwater budgets of the Persian Gulf, J. Geophys. Res., 108: C12-3391 doi:10.1029/2003JC001881.

Jordà, G., Gomis, D., Álvarez-Fanjul, E. and Somot S., (2012) Atmospheric contribution to Mediterranean and nearby Atlantic sea level variability under different climate change scenarios. Global and Planetary Change, 80: 198-214.
https://doi:10.1016/j.gloplacha.2011.10.013

Khedr AM, Abdelrahman SM, Tonbol KM. (2018). Sea level characteristics referenced to specific geodetic datum in Alexandria. World Acad Sci Eng Technol Int J Mar Environ Sci. 12: 78-86.
scholar.waset.org/1307-6892/10008544

P. Akbari, M. Sadrinasab, V. Chegini, M. Siadatmousavi. (2016). Tidal Constituents in the Persian Gulf, Gulf of Oman and Arabian Sea: a Numerical Study. Indian Journal of Geo-Marine Sciences 45: 1010-1016.

Pous, S., Carton, X. and Lazure, P., (2012) A Process Study of the Tidal Circulation in the Persian Gulf, Open J. Mar. Sci. 2: 131-140.

Prandle, D. (1991), Tides in estuaries and embayments , in Tidal Hydrodynamics, , John Wiley Toronto, Ont., pp.125–152،
Pugh, D. (1987) Tides, Surges and Mean Sea Level: A Handbook for Engineers and Scientists. Chichester, UK. John Wiley & Sons, 472 p.

Pugh, D.T. (1996) Tides, surges and mean sea-level, Chichester, UK. John Wiley & Sons, Ltd., 486pp.

Sultan, S.A.R., Ahmad, F., Elghribi, N.M., Al-Subhi, A.M., 1995. An analysis of Arabian Gulf monthly mean sea level. Cont. Shelf Res. 15:1471–1482
http://dx.doi.org/10.1016/0278-4343(94)00081-W

Svensson, C., Jones, D.A., (2004). Sensitivity to storm track of the dependence between extreme seas surges and river flows around Britain. Hydrology: Science and Practice for the 21st Century 1: 239-245.

Tonbol K., Shaltout M. (2013) Tidal and non-tidal sea level off Port Said. JKAU: Mar Sci. 24: 69–83.
V. C. John, (1992) Harmonic Tidal Current Constituents of the Western Arabian Gulf from Moored Current Measurements, Coastal Engineering, 17: 145-151.
doi:10.1016/0378-3839(92)90016-N